

Control a Contact Sensing Finger for Surface Haptic Exploration

Junghwan Back, João Bimbo, Yohan Noh, Lakmal Seneviratne, Kaspar Althoefer, Hongbin Liu*

Abstract— To efficiently explore a surface using the sense of touch, a novel contact sensing finger was created and a surface following control algorithm for the finger was devised. Based on the accurate estimation of contact locations, and the direction and magnitude of the normal and tangential forces, the finger can robustly and rapidly follow surfaces with large change in curvature while maintaining a desired constant normal force. In this paper, the design and testing of the contact sensing finger are presented and the control algorithm for surface contour following is proposed and validated using objects with different shapes and surface materials. The results demonstrate that using the developed finger and the control algorithm, a surface can be efficiently explored with rapid sliding speed. To demonstrate the potential applications of the proposed approach, the friction properties of an explored object surface are computed and, for a known object, its pose is estimated.

I. INTRODUCTION

Surface exploration through touch is an essential mechanism for humans to understand the physical properties of an unknown object, such as the surface roughness, object shape and compliance [1], [2]. Similarly, to allow a robot to autonomously work in unstructured environments, it is essential that the robot can perform efficient surface exploration to recognize the various attributes of the unknown environment with which it interacts. To date, numerous methods have been proposed to identify object surface properties through surface exploration. The uses of tactile sensors to classify the global shape of an object through multiple touches have been proposed in [3], [4], [5]. In [6], [2], a series of surface sliding strategies have been proposed to allow a dexterous robotic finger to recognize the object shape and to detect small surface features. To recognize surface textures, various methods of using a robotic finger to slide over a surface have been proposed, for example by analyzing the vibrations [7], [8], [9] or interaction forces [10].

One of the significant challenges to implement these aforementioned surface exploration methods for practical uses is the capability of controlling a robotic finger to adaptively and rapidly follow an unknown surface while maintaining a desired gentle force based on the sense of touch. A number of studies have applied force/position based control scheme for surface contour following. The limitation of this approach is that it either requires at least partial information of object shape or assumes the non-frictional sliding [11], [12], [13]. In addition, this approach has

difficulty to adapt to the rapid change in surface curvature and normally has slow execution speed. To improve the efficiency of surface following, a popular method is to use vision or proximity sensors to estimate and predict surface trajectories, such as the works done in [14], [15]. However the applications of these methods for robotic hand surface exploration are limited, due to the complexity of integrating proximity or vision sensors on the hand and the vision occlusions which is often generated. More recently, the study of surface contour following using a fingertip equipped with three axial tactile array sensors was introduced in [16].

This study shows that using distributed three-axial tactile information allows the finger to successfully follow an unknown shape. However the difficulty of developing miniaturized three-axial tactile array sensor and the slow excitation time of this method limit its applications. To allow a robot finger to rapidly and adaptively follow an unknown surface using the sense of touch alone, we propose a novel and efficient method for surface following control by using a contact sensing finger. In our previous work [10], a contact sensing fingertip has been developed with the capability to identify simultaneously the contact location and the direction and magnitude of the normal and tangential forces at a high frequency. In this paper, we developed a robotic finger integrated with the contact sensing fingertip and propose a surface following control scheme for utilizing the precise contact information obtained by the finger. Compared to existing methods, the advantages of the proposed method includes: 1) no prior knowledge of object shape is required and no restriction on surface friction level; 2) due to the accurate estimation of instantaneous normal and tangential force vectors provided by the fingertip, the surface following control is robust and adaptive to sudden geometry change of the surface shape; 3) the proposed control algorithm is simple and effective, thus allow rapid execution time; 4) only a force/torque is required for each finger, thus easy for practical implementation. The performance of the surface following control using the developed finger has been investigated using objects with different shapes and surface materials. The results demonstrate that the finger can successfully and rapidly follow all the surfaces while maintain a desired gentle normal force, even when the surface has a sharp change in curvature. The sliding speed of the finger can achieve >5 mm/s. The experiments show that from the controlled surface exploration, the finger is capable of estimating the friction properties of the object surface and also the pose of the object if the shape is known.

This work is supported by Grasp Stabilisation Control project funded by the TSB - Technology Strategy Board, UK. Junghwan Back, J. Bimbo, Y. Noh, L.D. Seneviratne K. Althoefer and H. Liu are with Department of Informatics, King's College London, UK, WC2R 2LS.

*indicates the correspond author, email{ hongbin.liu@kcl.ac.uk }

II. THE CONTACT SENSING FINGER

A. Finger Design

To effectively conduct surface haptic exploration, a robotic finger was developed, with three links and two revolute joints, as shown in Fig. 1. This finger equipped with a contact sensing fingertip which is capable of accurately estimating the instantaneous friction force and the normal force without the prior knowledge of the surface geometry. The algorithm for computing such information is introduced in detail in [10]. The fingertip consists of a 6-axis force/torque sensor (ATI Nano17, resolution 0.003 N) and a hemispherical hat as shown in Fig. 1. The fingertip was made of the ABS (Acrylonitrile butadiene styrene) plastic material and has a diameter of 20 mm.

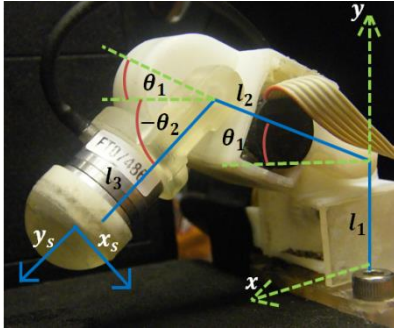


Figure 1. The developed Contact sensing finger

Each joint of the finger possesses a DC motor (Faulhaber U1512, with 324 gear ratio) and two gears (32 teeth, and 12 teeth), resulting a total gear ratio of 864. The DC motor driver receives velocity input values from the Simulink model and outputs encoder values using serial communication between the driver and the host computer, an Intel i5 CPU 3.2GHz, and 4GB RAM. The Simulink model on the host computer reads the output of the force-torque sensor via a National Instruments (NI) PCIe-6320 data acquisition card.

B. Computing of Contact Information

The information provided by the developed finger includes the contact location on fingertip in finger base frame of reference and the instantaneous normal and tangential force vectors. Normal and tangential forces are calculated based on the estimation of the contact location on the fingertip in the force/torque sensor reference frame. The contact equilibrium system equation proposed in [17] is used to calculate the contact location based on force/torque measured.

$$g(x) = \begin{cases} k\nabla s_1 - f_y z + f_z y - m_x \\ k\nabla s_2 - f_z x + f_x z - m_y \\ k\nabla s_3 - f_x y + f_y x - m_z \\ S(x, y, z) \end{cases} \quad (1)$$

Eq. (1) shows the system of equations to be solved. $k\nabla s_n$ is the local torque, and f and m are the forces and moments measured on the sensor. S is the surface equation. The solution to these equations is found iteratively, using the

Levenberg-Marquardt method (LMA), as suggested in Liu et al [10]. Once the x-y-z coordinates of the contact location are computed, the normal vector Q on that point can be calculated as $\nabla S(x, y, z)$, and the normal component of that force is the projection of the resultant force on that normal vector, calculated using (2). The tangential component is then calculated using (3).

$$F_n = \frac{Q^T F}{Q^T Q} Q \quad (2)$$

$$F_t = \sqrt{\frac{1 - \cos^2 \left(\frac{F_n}{\|F\|} \right)}{\cos \left(\frac{F_n}{\|F\|} \right)}} F_n \quad (3)$$

Applying the above algorithm, the contact information is obtained at the frequency of 543 Hz. To validate the accuracy of the contact location estimation, the fingertip was marked at 9 points as shown in Fig. 3. A caliper was used to contact the centre locations of two corresponding markers sequentially. The distance between the two contact locations identified by the algorithm is compared with the caliper's reading. The results are shown in Table I. It was found that the mean error was 0.41mm, indicating a high accuracy in contact location estimation.

TABLE 1. VALIDATION OF CONTACT LOCATION ACCURACY

Number	Distance from Caliper	Distance from Sensor	Error
1	10.854 mm	10.8561mm	0.021mm
2	11.84 mm	11.6297mm	0.22103mm
3	17.74 mm	16.7735mm	0.9665mm
4	18.73 mm	19.1651mm	0.4351mm

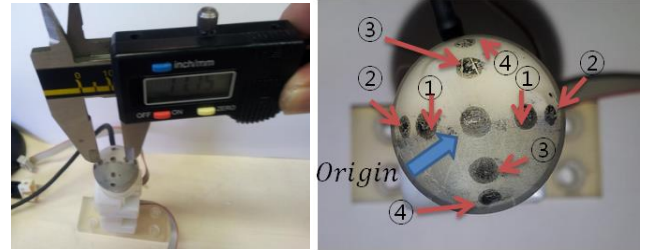


Figure 2. Examination for accuracy for contact location estimation

Validation of the estimation of normal and tangential forces is done by using a benchmarking force-torque sensor, pressed flat against the surface, the same procedure as described in [10]. The normal force on the fingertip should be equal to the z-axis force on the benchmarking sensor, and the tangential force on the fingertip should be equal to the norm of the resultant x and y-axis forces on benchmarking sensor. The maximum errors of normal and tangential forces were 0.075 and 0.08 Newton respectively, which is comparable to the sensor's noise level.

III. SURFACE FOLLOWING CONTROL ALGORITHM

As aforementioned, the effective surface exploration requires both force and position control [4], since forces generated by the surface contact are coupled with the velocity and the position of fingertip. In this paper a position controller is developed to work in parallel with a force controller which provides desired contact normal or tangential forces. Joint encoder values, magnitude and direction of forces are utilized as the feedback to the controller. In some situations, the fingertip cannot reach desired locations because of the resistance force generated by the material surface, resulting undesired overshoot and undershoot. This implies that an automatic PID gain values adjustment algorithm is required. This however, requires high precision control, which is often inconvenient. In view of this limitation, a PD controller is proposed in this paper to achieve the velocity control using desired velocity ratios between the finger joints. It can be proven that fingertip trajectory is decided by the ratios between the velocities of individual joints irrespective of absolute velocities (see Appendix for the proof).

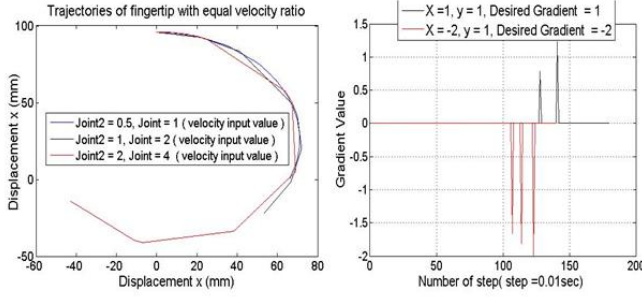


Figure 3. Trajectory Analysis (a) trajectories with velocity ratio 2:1;(b) gradients on desired x,y location (start location was (0,0), and desired direction (x,y))

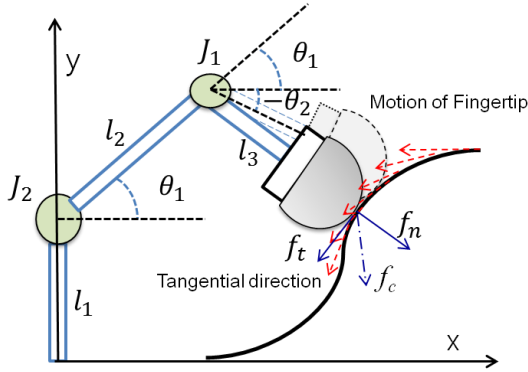


Figure 4. The schematic drawing of the control algorithm for surface contour following

The velocity ratio controller initially plans a trajectory which intersects with the object surface. After the finger is in contact with the surface, force feedback is used to continuously adjust the velocity ratio of finger joints to allow smooth surface following. As shown in Fig.4, the finger attempts to move along the tangential direction of the surface. Meanwhile, the finger's position is adjusted along the normal direction to reach a desired normal contact force. The P gain was chosen so that the angular rotation of each joint is one degree per sample time under the initial voltage level and

zero-load. Role of D gain is to suppress the sharp deviation of normal force with respect to the reference. The D gain is adaptive depending on contact condition.

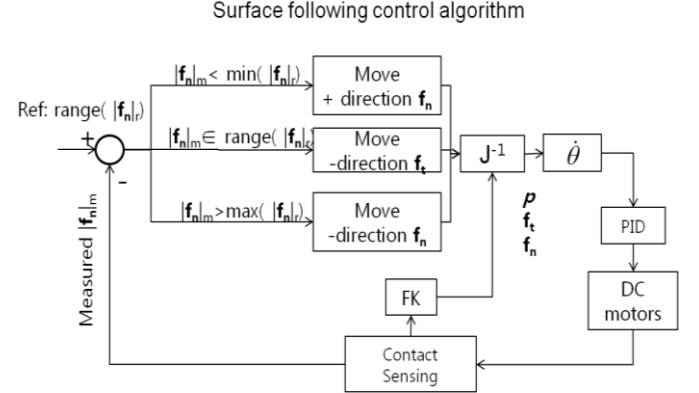


Figure 5. The control diagram for surface contour following using the contact sensing finger

The control diagram of the surface following is illustrated in Fig.5. The current location of the fingertip is calculated with the forward kinematics, using each joint's encoder value as shown below, in (4), where c_i and s_i are short for $\cos(\theta_i)$, and $\sin(\theta_i)$, respectively and l_i are the link lengths of the robot.

$$\begin{aligned} x &= l_3 C_1 C_2 - l_3 S_1 S_2 + l_2 C_1 + x_s \\ y &= l_3 S_1 C_2 + l_3 C_1 S_2 + l_2 S_1 + l_1 + y_s \end{aligned} \quad (4)$$

The each joint's angle is limited: for joint 1, $0 \leq \theta_1 \leq \frac{\pi}{2}$ and for joint 2, $-\frac{\pi}{2} \leq \theta_2 \leq 0$. x_s and y_s are the contact locations on the fingertip. Then, the desired next position x_n , y_n of the fingertip are given by the direction of the tangential forces \hat{x}_t , \hat{y}_t , as shown in 5.

$$\begin{aligned} x_n &= x + \hat{x}_t \\ y_n &= y + \hat{y}_t \end{aligned} \quad (5)$$

$$\theta_{2n} = \cos^{-1} \left[\frac{x^2 + y^2 - l_2^2 - l_3^2}{2l_2 l_3} \right] \quad (6)$$

$$\theta_{1n} = \cos^{-1} \left[\frac{-y l_3 S_2 - (l_3 C_2 + l_2)x + l_3 l_2 C_2}{(-l_3^2 S_2^2) - (l_3 C_2 + l_2)^2} \right] \quad (7)$$

The angle of joint 2 is determined first using (6). Once the next θ_2 is determined, the value of θ_1 in next step can be formulated using the inverse kinematics model as (7). Once the current θ_1 , θ_2 and the angular positions θ_{1n} , θ_{2n} of the next step are known, we can calculate the velocity ratio as shown in 8.

$$\begin{aligned} \text{if } v_1 > 0, \quad \varepsilon_1 &= \frac{\theta_{1n}}{\theta_1}, \text{ else } \varepsilon_1 = \frac{\theta_1}{\theta_{1n}}, \\ \text{if } v_2 < 0, \quad \varepsilon_2 &= \frac{\theta_{2n}}{\theta_2}, \text{ else } \varepsilon_2 = \frac{\theta_2}{\theta_{2n}}, \end{aligned} \quad (8)$$

The values of ε_1 and ε_2 are fed into the PD controller directly. These values are modified according to the normal and tangential force vectors. When the normal force is outside the reference range of force, the fingertip follows the normal

direction to adjust the normal force, as in (9).

$$\hat{x}_t = \frac{F_{nx}}{\|F_n\|}, \quad y_t = -\frac{F_{ny}}{\|F_n\|} \quad (9)$$

if $F_n < \min(ran) : \hat{x}_t = -\hat{x}_t$
 $\hat{y}_t = -\hat{y}_t$

Otherwise, when the normal force is inside the range of $0.8N \leq F_n \leq 1.2N$, the controller drives the finger along the tangential force direction as in (10).

$$\hat{x}_t = \frac{F_{tx}}{\|F_t\|}, \quad y_t = \frac{F_{ty}}{\|F_t\|} \quad (10)$$

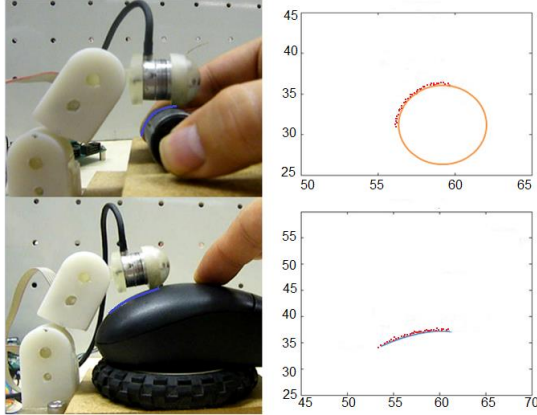


Figure 6. Surface following on different objects. The dots plot the recorded contact trajectory

The developed surface following controller has been implemented and achieved a very good performance. It was found that the finger can rapidly and robustly follows an unknown shape, Fig. 6. During the surface following, the normal force is capable to maintain almost constantly at the desired level, Fig. 7.

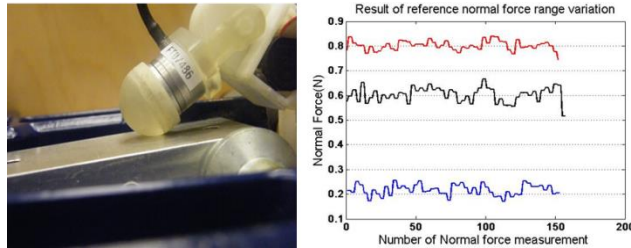


Figure7. Surface following while maintaining a constant normal force. Three different ranges of normal force were applied: (0.8-0.9), (0.6-0.7), (0.2 - 0.3), units are in "N"

IV. FINGER CONTROL FOR SURFACE HAPTIC EXPLORATION - APPLICATIONS

The algorithm for surface exploration is built in Matlab Simulink. The finger is attached to the end effector of a Mitsubishi RV-6SL robot arm which is controlled using the Robot Operating System (ROS) on a separate computer. The finger and the arm are synchronized and communicate via a UDP communication socket, and the system is shown in Fig. 10. The two main objectives of surface exploration experiments include surface friction properties recognition and pose estimation of the target object. During the

exploration, the finger slides over an unknown shape following 5 to 7 different paths; the normal force is maintained at range of 0.6-0.7 N. In total, eight different objects were investigated.

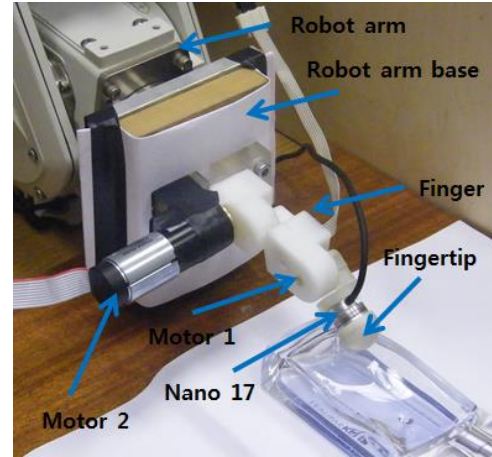


Figure 8. Experimental setup

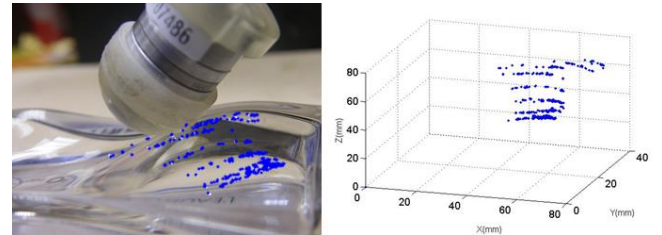


Figure 9. Exploration of a perfume bottle

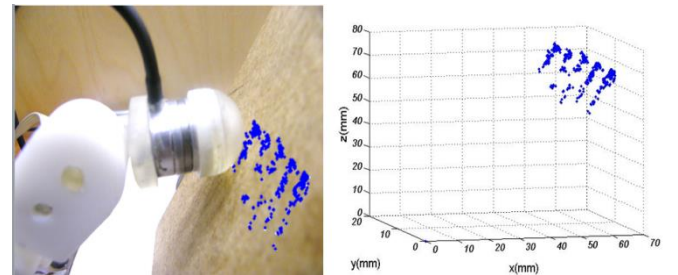


Figure 10. Exploration of a float wooden board

A. Friction Properties Acquisition

Given the ability of the proposed system to measure normal and tangential forces during an exploration task, the friction ratio between these forces (F_t/F_n) can be evaluated. While the finger is stroking an object, this ratio will not exceed the static friction coefficient of each material [18], [19], [10].

In the experiments carried out, objects with different surface materials were tested and the friction ratios obtained are plotted in Fig. 11. This allowed the identification of the stroked object, among a database of eight objects (rubber ball, rubber tape, steel slab, aluminium can, aluminium bottle computer mouse, perfume glass and wooden board). The results are expressed in Table II. This information can provide clues to recognize the surface material and also for object identification, in case there exists previous knowledge of existing objects.

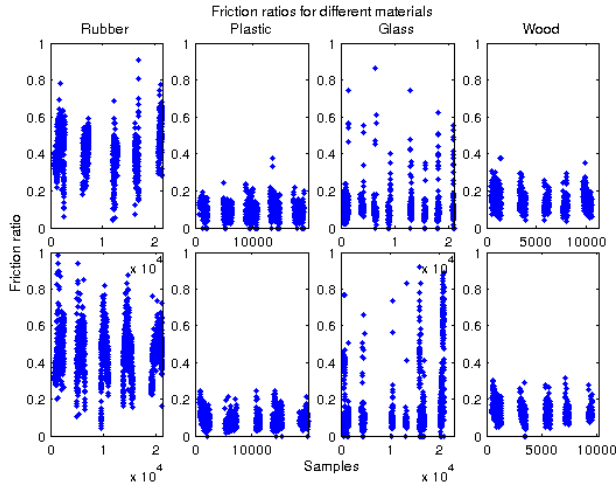


Figure 11. Friction ratios during strokes on different materials. Two strokes on each material are displayed.

B. Object Pose Estimation From Exploration

After the identification of the explored object, the spatial location of each contacted point on the surface can be recorded, taking into account the contact location on the fingertip, the forward kinematics of the finger and the pose of the robot arm end-effector where the finger is attached, as shown previously in Fig. 10.

TABLE II. VALIDATION OF COEFFICIENT OF FRICTION

Object	Coefficient of Friction	Object	Coefficient of Friction
Rubber ball	0.5185	Aluminium can	0.1510
Rubber tape	0.2275	Perfume case(glass)	0.1097
Wood flat	0.2291	Mouse(plastic)	0.0974
Steel flat	0.1490	Aluminium bottle	0.1218

This contact information can provide an estimate of the object's current pose by fitting the object's known geometric shape to the finger surface trajectories [20]. One method of fitting these two sets of points is the Iterative Closest Point (ICP) [21]. A transform is found on the object such that the mean-square distances are minimised. In this paper, Kjer's Matlab implementation of ICP was used [22], and yielded the results shown in Fig. 12 and 13 for a computer mouse and a flat wooden board respectively. These results show that the proposed exploration strategy allows the tracking of an object's surface, enabling the estimation of a known object's pose. In Fig. 13 the estimation cannot accurately detect where on the board it is touching. This is because in this particular object, the points collected during the exploration task could fit anywhere on the two larger sides of the board. Despite this limitation, the 3D orientation of the object is correctly identified.

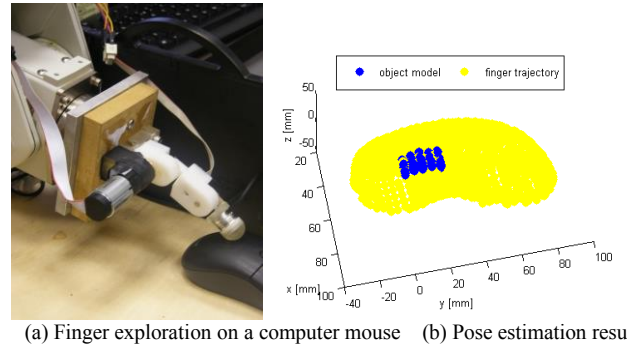


Figure 12. Results for the computer mouse exploration

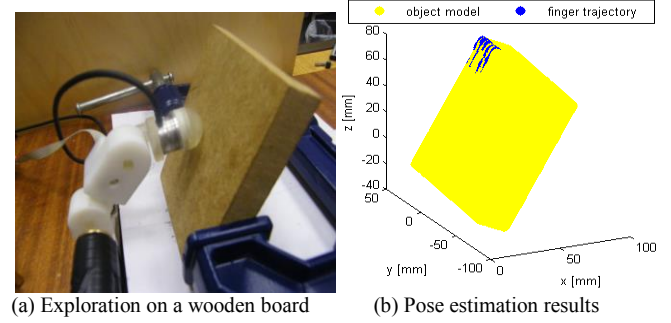


Figure 13. Results for a flat wooden board

The fitting errors for both fittings are shown in Fig. 14. After 30 iterations, the mean error for the computer mouse and for the wooden board fitting were respectively 1.419 mm and 0.7931 mm.

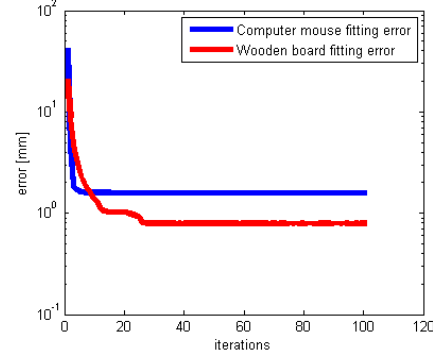


Figure 14. Fitting errors for the ICP algorithm after 100 iterations. (Note the log scale)

V. CONCLUSIONS AND FUTURE WORK

This paper presented a robotic finger and a control algorithm to have it explore an object's surface maintaining contact with a reasonably constant normal force. The control strategy is based on velocity ratio control between the two joints of the finger. It uses the contact information (contact location and normal and tangential forces) provided by a six-axis force-torque sensor mounted on a fingertip. The proposed strategy was proved successful in different surfaces and geometries. To illustrate the advantages of this exploration method, two applications were presented where the finger was able to explore the surface to obtain friction information and, given the set of contact points obtained

during the exploration task, to have a good estimate of the object's position and orientation.

Further developments of this system include the recognition of the object based not only on its friction properties but also on the local geometries detected. The exploration could also be intelligently driven to look for particular features and to follow them, such as edges, handles and buttons.

APPENDIX

Proposition: The trajectory of the fingertip (regardless of time) is only dependent on the velocity ratio between two finger joints

Proof: Given the velocity ratio between two joints are constant, the following equation hold, where $\dot{\theta}_{1,2}$, and $\hat{\theta}_{1,2}$ are the different angular velocity sets.

$$\frac{\dot{\theta}_1(t)}{\dot{\theta}_2(t)} = \frac{\hat{\theta}_1(t)}{\hat{\theta}_2(t)} = \lambda \quad (11)$$

Rearrange Eq.11, the following relationship holds,

$$\frac{\dot{\theta}_1(t)}{\hat{\theta}_1(t)} = \frac{\dot{\theta}_2(t)}{\hat{\theta}_2(t)} = \alpha(t) \quad (12)$$

Given the position of the fingertip is a function of the two joint angles, i.e. $\mathbf{p} = \mathbf{G}(\theta_1, \theta_2)$, where \mathbf{p} is position, we need to prove that if $\theta_1(T) = \hat{\theta}_1(K)$, where T and K are the different time, then $\theta_2(T) = \hat{\theta}_2(K)$.

$$\text{Let } \theta_1(T) = \int_0^T \dot{\theta}_1(t)dt \text{ and } \hat{\theta}_1(K) = \int_0^K \hat{\theta}_1(t)dt \quad (13)$$

From Eq.13, we obtain

$$\hat{\theta}_1(K) = \int_0^K \frac{1}{\alpha(t)} \dot{\theta}_1(t)dt = \int_0^T \dot{\theta}_1(t)dt \quad (14)$$

$$\text{Let } \theta_2(T) = \frac{1}{\beta} \int_0^T \dot{\theta}_2(t)dt \quad (15)$$

From Eq.11, we obtain,

$$\theta_2(T) = \frac{1}{\beta} \int_0^T \dot{\theta}_1(t)dt \quad (16)$$

$$\hat{\theta}_2(K) = \int_0^K \frac{1}{\beta} \frac{1}{\alpha(t)} \dot{\theta}_2(t)dt = \frac{1}{\beta} \int_0^K \frac{1}{\alpha(t)} \dot{\theta}_1(t)dt \quad (17)$$

$$\text{Since } \int_0^K \frac{1}{\alpha(t)} \dot{\theta}_1(t)dt = \int_0^T \dot{\theta}_1(t)dt \quad (18)$$

Thus, $\hat{\theta}_2(K) = \theta_2(T)$. Hence the trajectory is determined only by the velocity ratio and the statement is proved.

REFERENCE

- [1] R. L. Klatzky, S. J. Lederman, and V. a. Metzger, "Identifying Objects by touch: an "expert system", " *Perception & psychophysics*, vol. 37, no. 4, pp. 299–302, Apr 1985.
- [2] M. Okamura, and R. Cutkosky, "Feature Detection for Haptic Exploration with Robotic Fingers," *The International Journal of Robotics Research*, vol. 20, no. 12, pp. 925–938, Dec 2001.
- [3] H. Liu, X. Song, T. Nanayakkara, L.D. Seneviratne, K. Althoefer, "A computationally fast algorithm for local contact shape and pose classification using a tactile array sensor", in *Proceedings of IEEE International Conference on Robotics and Automation (ICRA)*, pp. 1410-1415, 2012.
- [4] M. Meier, M. Schopfer, R. Haschke, and H. Ritter, "A Probabilistic Approach to Tactile Shape Reconstruction," *IEEE Transactions on Robotics*, vol. 27, no. 3, pp. 630–635, June 2011.
- [5] N. Gorges, S. E. Navarro, D. G'oger, and H. W'orn, "Haptic object recognition using passive joints and haptic key features," in *2010 IEEE Int. Conf. on Robotics and Automation*, pp. 2349–2355, May 2010.
- [6] A. Okamura, M. Turner, and M. Cutkosky, "Haptic exploration of objects with rolling and sliding," in *Proc. IEEE Int. Conf. on Robotics and Automation*, vol. 3, pp. 2485–2490, Apr 1997.
- [7] M. Tanaka, J. L. Leveque, H. Tagami, K. Kikuchi, and S. Chonan, "The "Haptic Finger"- a new device for monitoring skin condition," *Skin Research and Technology*, vol. 9, no. 2, pp. 131–136, Jan 2003.
- [8] K. Hosoda, Y. Tada, and M. Asada, "Anthropomorphic robotic soft fingertip with randomly distributed receptors," *Robotics and Autonomous Systems*, vol. 54, no. 2, pp. 104–109, Feb 2006.
- [9] N. Jamali and C. Sammut, "Majority Voting: Material Classification by Tactile Sensing Using Surface Texture," *IEEE Transactions on Robotics*, vol. 27, no. 3, pp. 508–521, June 2011.
- [10] H. Liu, X. Song, J. Bimbo, L. Senerivatne, and K. Althoefer, "Object Surface Material Recognition through Haptic Exploration using an Intelligent Contact Sensing Finger," in *Proceedings of IEEE/RSJ Int. Conf. on Intelligent Robots and Systems (IROS' 2012)*, Oct 2012.
- [11] U. Nunes, P. Faia, and A. T. de Almeida, "Sensor-based 3-D autonomous contour-following control," in *Proc. IEEE/RSJ Int. Conf. on Intelligent Robots and Systems IROS'94*, vol. 1. IEEE, pp. 172–179, Sep 1994.
- [12] K. Kiguchi and T. Fukuda, "Position/force control of robot manipulators for geometrically unknown objects using fuzzy neural networks," *IEEE Transactions on Industrial Electronics*, vol. 47, no. 3, pp. 641–649, June 2000.
- [13] D. Bossert, U.-L. Ly, and J. Vagners, "Experimental evaluation of a hybrid position and force surface following algorithm for unknown surfaces," in *Proceedings of IEEE International Conference on Robotics and Automation*, vol. 3, pp. 2252–2257, Apr 1996.
- [14] J. Baeten and J. De Schutter, "Hybrid vision/force control at corners in planar robotic-contour following," *IEEE/ASME Transactions on Mechatronics*, vol. 7, no. 2, pp. 143–151, June 2002.
- [15] H. Koch, A. Konig, K. Kleinmann, A. Weigl-Seitz, and J. Suchy, "Predictive robotic contour following using lasercamera-triangulation," in *2011 IEEE/ASME International Conference on Advanced Intelligent Mechatronics (AIM)*, pp.422–427 July 2011.
- [16] M. Ohka, J. Takata, H. Kobayashi, H. Suzuki, N. Morisawa, and H. B. Yussuf, "Object exploration and manipulation using a robotic finger equipped with an optical three-axis tactile sensor," *Robotica*, vol. 27, no. 05, p. 763–770, Nov 2008.
- [17] A. Bicchi, J. K. Salisbury, and D. L. Brock, "Contact Sensing from Force Measurements," *The International Journal of Robotics Research*, vol. 12, no. 3, pp. 249–262, June 1993.
- [18] X. Song, H. Liu, T. Nanayakkara, K. Althoefer, L. Seneviratne, "Efficient Break-Away Friction Ratio and Slip Prediction Based on Haptic Surface Exploration", *IEEE Transactions on Robotics*, vol 30,no.1, pp.203-219, 2014.
- [19] H. Liu, X. Song, T. Nanayakkara, K. Althoefer, L. Seneviratne, "Friction estimation based object surface classification for intelligent manipulation," *Workshop on Autonomous Grasping at IEEE International Conference on Robotics and Automation*, 2011.
- [20] J. Bimbo, H. Liu, L. Seneviratne, and K. Althoefer, "Combining Touch and Vision for the Estimation of an Object's Pose During Manipulation," in *Proceedings of IEEE/RSJ International Conference on Intelligent Robots and Systems (IROS'2013)*, Nov 2013.
- [21] P. J. Besl and N. D. McKay, "A method for registration of 3-D shapes," *IEEE Transactions on Pattern Analysis and Machine Intelligence*, vol. 14, no. 2, pp. 239–256, Feb 1992.
- [22] H. M. Kjer and J. Wilm, "Evaluation of surface registration algorithms for PET motion correction," Bachelor's thesis, Technical University of Denmark, DTU, DK-2800 Kgs. Lyngby, Denmark, 2010.